ORIGINAL ARTICLE

Molecular Classification of Neuroendocrine Tumors of the Thymus

Helen Dinter,[a] Hanibal Bohnenberger, MD,[a] Julia Beck, PhD,[b] Kirsten Bornemann-Kolatzki,[b] Ekkehard Schütz, MD,[b] Stefan Küffer,[a] Lukas Klein,[a] Teri J. Franks, MD,[c] Anja Roden, MD,[d] Alexander Emmert, MD,[e] Marc Hinterthaner, MD,[e] Mirella Marino, MD,[f] Luka Brcic, MD,[g] Helmut Popper, MD,[g] Cleo-Aron Weis, MD,[h] Giuseppe Pelosi, MD,[i] Alexander Marx, MD,[h] Philipp Ströbel, MD[a,*]

[a]*Institute of Pathology, University Medical Center Göttingen, Göttingen, Germany*
[b]*Chronix Biomedical, Göttingen, Germany*
[c]*Pulmonary & Mediastinal Pathology, The Joint Pathology Center, Silver Spring, Maryland*
[d]*Department of Laboratory Medicine and Pathology, Mayo Clinic, Rochester, Minnesota*
[e]*Department of Thoracic and Cardiovascular Surgery, University Medical Center, Georg-August University, Göttingen, Germany*
[f]*Department of Pathology, IRCCS Regina Elena National Cancer Institute, Rome, Italy*
[g]*Diagnostic and Research Center, Institute of Pathology, Medical University of Graz, Graz, Austria*
[h]*Institute of Pathology, University Medical Center Mannheim, University of Heidelberg, Germany*
[i]*Department of Oncology and Hemato-Oncology, University of Milan, and Inter-Hospital Pathology Division, IRCCS MultiMedica, Milan, Italy*

Received 14 January 2019; revised 26 March 2019; accepted 22 April 2019
Available online - 28 April 2019

ABSTRACT

Introduction: The WHO classification of pulmonary neuroendocrine tumors (PNETs) is also used to classify thymic NETs (TNETs) into typical and atypical carcinoid (TC and AC), large cell neuroendocrine carcinoma (LCNEC), and small cell carcinoma (SCC), but little is known about the usability of alternative classification systems.

Methods: One hundred seven TNET (22 TC, 51 AC, 28 LCNEC, and 6 SCC) from 103 patients were classified according to the WHO, the European Neuroendocrine Tumor Society, and a grading-related PNET classification. Low coverage whole-genome sequencing and immunohistochemical studies were performed in 63 cases. A copy number instability (CNI) score was applied to compare tumors. Eleven LCNEC were further analyzed using targeted next-generation sequencing. Morphologic classifications were tested against molecular features.

Results: Whole-genome sequencing data fell into three clusters: CNI_{low}, CNI_{int}, and CNI_{high}. CNI_{low} and CNI_{int} comprised not only TC and AC, but also six LCNECs. CNI_{high} contained all SCC and nine LCNEC, but also three AC. No morphologic classification was able to predict the CNI cluster. Cases where primary tumors and metastases were available showed progression from low-grade to higher-grade histologies. Analysis of LCNEC revealed a subgroup of intermediate NET G3 tumors that differed from LCNEC by carcinoid morphology, expression of chromogranin, and negativity for enhancer of zeste 2 polycomb repressive complex 2 subunit (EZH2).

Conclusions: TNETs fall into three molecular subgroups that are not reflected by the current WHO classification. Given the large overlap between TC and AC on the one hand, and AC and LCNEC on the other, we propose a

*Corresponding author.

Drs. Dinter and Bohnenberger contributed equally to this work.

Disclosure: Dr. Brcic has received grants from Astra Zeneca; has received personal fees from Roche, Astra Zeneca, and MSD; and has received nonfinancial support from Roche, Pfizer, Astra Zeneca, MSD, and Abbvie.

Address for correspondence: Philipp Ströbel, MD, Institute of Pathology, University Medical Center Göttingen, Robert-Koch-Str. 40, D-37075 Göttingen, Germany. E-mail: philipp.stroebel@med.uni-goettingen.de

ISSN: 1556-0864

https://doi.org/10.1016/j.jtho.2019.04.015

morphomolecular grading system, Thy-NET G1-G3, instead of histologic classification for patient stratification and prognostication.

Keywords: Neuroendocrine; Carcinoid; Thymus; Molecular; Genetic; Classification

Introduction

Neuroendocrine tumors (NETs) have been described in many organs, but are most common in the gastroenteropancreatic (GEP-NET) and pulmonary tract (PNET). In comparison, thymic neuroendocrine tumors (TNETs) are rare, accounting for less than 5% of mediastinal and thymic neoplasms, and 0.4% of all neuroendocrine tumors overall.[1-4] TNETs and PNETs are classified using the same WHO criteria into low-grade typical carcinoids (TCs), intermediate-grade atypical carcinoids (ACs), and two high-grade malignancies, large cell neuroendocrine carcinoma (LCNEC) and small cell carcinoma (SCC). All four tumors require neuroendocrine morphology by light microscopy (organoid nesting, rosette formation, peripheral palisading of tumor nests, and trabeculae), and ultrastructural or immunohistochemical evidence of neuroendocrine differentiation for separation from other tumors. Within the four tumors, TC is defined as having less than two mitoses per 2 mm^2, no necrosis, and size of 0.5 cm or greater, whereas AC is defined as having two to 10 mitoses per 2 mm^2 and/or necrosis. LCNEC requires non–small cell morphology, SCC requires small cell morphology, and both require greater than 10 mitoses per 2 mm^2. Ki-67 is often used as an ancillary stain, but is not a formally recognized criterion. Although the WHO classification is based on morphology, the inclusion of metric criteria implies that it is also a grading system.[5] In contrast, the current European Neuroendocrine Tumor Society (ENETS)/WHO classification of GEP-NET uses metric criteria based on mitotic count and Ki-67 index to grade tumors that are separated into NET and neuroendocrine carcinoma by morphology.[6] GEP-NETs are thus classified into NET G1, NET G2, and large-cell and small-cell NEC. More recently, an additional category of "NET G3" has been introduced in GEP-NET.[7] These NET G3 are characterized by a well differentiated (carcinoid) morphology, whereas the Ki-67 index indicates G3.[7] In an attempt to reconcile difficulties of morphologic classifications with current knowledge about the biology and behavior of PNET, and to separate more clearly morphologic and metric criteria, Pelosi et al.[5] have proposed an integrated classification of PNET into Lu-NET G1 – G3 based on morphology, amount of necrosis, mitotic count, and Ki-67 index.[5]

Despite an emerging unifying concept of NETs across all organs, the anatomic site is biologically important because tumors of different anatomic location behave differently and show divergent risk factors (e.g., the role of smoking habits), clinical presentation, and molecular features.[8,9] Although thoracic NET (PNET and TNET) are often referred to as foregut NET and have traditionally been classified using the same criteria, there are clinicopathologic and genetic differences. For example, AC and LCNEC are the most frequent subtypes in the thymus, whereas TC and SCC prevail in the lung. Furthermore, the correlation between genotype and phenotype in patients with menin 1 (MEN1) is reported to be lower in TNET, and the genetic profile of thymic carcinoids differs from pulmonary carcinoids.[10-16] On the other hand, the current WHO classification has shown clinical relevance and reflects genetic alterations found in TNET.[16]

Whereas the diagnosis of TC, AC, and SCC is usually straightforward, LCNEC is more problematic. The WHO classification states that some LCNEC have carcinoid morphology, but exceed the mitotic count accepted for AC. Under this definition, LCNEC is likely to comprise a large spectrum of tumors that overlap with AC at the one end and with SCC at the other. A recent small case series even provides genetic evidence that some thymic LCNEC may develop from AC.[17] Based on retrospective clinical data, we previously reported that a cutoff at 15 mitoses separated TNET with an increased risk of recurrence.[16] At the other end of the spectrum and regarding the distinction from SCC, we and others found a better prognosis for LCNEC than SCC, which may again be due to the fact that the current WHO definition of LCNEC embraces a spectrum of heterogenous tumors with very different prognoses.[16,18] However, a subgroup of NET G3 tumors with intermediate biological behavior has so far not been described in the thymus.

We reasoned that molecular features such as gene copy number variations might give valuable insights into TNET biology and might provide guidance on how to best classify them. We therefore examined the molecular features of a large retrospective series of TNET and compared the results to different histologic classification systems to establish robust criteria that allow better stratification of these rare tumors.

Materials und Methods

Patients and Tumor Specimens

For this study, we used archival formalin-fixed, paraffin-embedded (FFPE) tissue slides or blocks of

107 TNETs from 103 patients collected between 1996 and 2016. Seventy-three cases had been previously described in another study.[16] Cases were contributed from centers in Germany (Göttingen and Mannheim), Austria (Graz), Italy (Rome), and the United States (Silver Spring, Maryland, and Rochester, Minnesota). The study was performed with approval from the University Medical Center Göttingen ethics committee (no. Dok_7_2016). Materials included resection specimens and biopsy specimens. In a few cases, there was more than one specimen from a given patient. Case #1 had a primary tumor and a synchronous metastasis. Case #2 had a primary tumor and a metachronous metastasis 3 years later. Case #3 had two samples of the primary tumor and one metachronous metastasis 5 years later. Case #4 had two samples of the primary tumor. All cases were carefully reviewed by two pathologists (H.D. and P.S.) and classified according to the WHO 2015 classification scheme.[1] Mitotic counts were determined in 10 high-power field (HPF) on hematoxylin and eosin–stained sections, using an Olympus BX53 microscope (40× objective, field-of-view diameter of 0.55 mm, resulting in 10 HPF = 2.37 mm^2). Only unequivocal mitoses (i.e., identifiable spindles) were counted. After final review, 22 cases were classified as TC, 51 cases as AC, 28 as LCNEC, and 6 cases as SCC (Table 1). The same cases were also classified according to the ENETS/WHO classification for GEP-NET into NET G1, NET G2, LCNEC, and SCC, and according to the PNET classification proposed by Pelosi et al.[5] into G1, G2, and G3.[5,6] The Ki-67 index was determined using immunohistochemical stains that were analyzed using morphometric digital image analysis (see below). In cases where this analysis was technically not feasible, a photograph of a representative hot spot was taken at 400× magnification, printed out, and positive versus negative tumor cell nuclei were manually counted.

Immunohistochemistry

Immunohistochemistry (IHC) was performed after antigen retrieval on a Dako Autostainer platform using Dako EnV FLEX Peroxidase as the detection system. All stains were performed using standard protocols. Antibodies included synaptophysin (Dako/Agilent, Hamburg, Germany, clone DAK-Synap, ready-to-use), chromogranin (CellMarque, Rocklin, CA, clone LK2H10, ready-to-use), Ki-67 (Dako/Agilent, clone MIB-1, 1:200), ATRX (ThermoFisher, clone CLO 537, 1:100), DAXX (Sigma, clone HPA 008736, 1:200), SSTR2A (Zytomed Systems, Berlin, Germany, rabbit polyclonal, 1:100), RB (Sigma, rabbit polyclonal, 1:100), P53 (Dako, clone DO-7, ready-to-use), and EZH2 (Leica, Wetzlar, Germany, clone 6A10, 1:50). Immunohistochemical stains were evaluated using a three-tiered scoring system for staining intensity (0 = negative, 1 = weakly positive, and 2 = strongly positive) and the percentage of positively stained tumor cells (<25% positive cells, 25% to 50% positive cells, >50% positive cells). For statistical evaluation, cases that had at least 25% cells with either weak or strong staining intensity were counted as positive.

Morphometric Image Analysis of Ki-67 Stains

The number on non-stained and stained cells in Ki-67 IHC was evaluated by a custom written image processing MATLAB-tool (Mathworks, Natick, Massachusetts): first, background and foreground staining are separated in 3-dimensional color space. Second, by means of a dilation-

Table 1. Clinical Details of 107 TNET Patients

	Cases (n)	*Sex (M/F)*	*Age Range, y (Median)*	*Status (Alive/Dead)*	*Median Survival, mo*	*Treatment*	*Tumor Size Range, cm (Median)*
TC	22	17/5	8-78 (57)	6/1	48	S: 4 C: 1 S + R: 2	2.9-12 (11)
AC	51	44/7	18-85 (54)	18/13	59	S: 11 S + C: 2 S + R :9 C + R: 1 S + C + R: 7	1-25 (8)
LCNEC	28	16/12	16-79 (57.5)	2/8	30	S: 3 C: 1 S + C: 1 S + C + R: 2	6-20 (12)
SCC	6	5/1	34-74 (58.5)	0/3	1	S + C: 2	12-15 (12)

TC, typical carcinoid; AC, atypical carcinoid; LCNEC, large cell neuroendocrine carcinoma; SCC, small-cell carcinoma; S, surgery, C, chemotherapy; R, radiotherapy; TNET, thymic neuroendocrine tumor; M, male; F, female.

erosion sequence, overlapping nuclei are separated and subsequently counted. The tool was tested and validated by comparison to manual count based ground truth ($r^2 = 0.87$ for the validation group).

Shallow Whole-Genome Sequencing and Chromosomal Instability Score

DNA was extracted from FFPE tissue blocks using the InnuPREP FFPE DNA Kit on the InnuPure C16 System (Jena Analytika, Jena, Germany) according to manufacturer instructions. Molecular analysis was possible in 63 tumor samples (13 TC, 30 AC, 16 LCNEC, and 4 SCC).

Extracted DNA was ultrasonically sheared to an approximate fragment size of 200 bp using a Covaris S2 focused-ultrasonicator. Sequencing libraries were prepared using the NEBNext Ultra II DNA Library Preparation Kit for Illumina (New England Biolabs, Frankfurt, Germany) according to the manufacturer instructions. Paired-end sequencing (37/38 bp) was conducted on an Illumina NextSeq500 with base calling using the bcl2fastq program version 2.17.1.14. An average of 20.2 million (standard deviation: 5.5 million) reads were generated per sample. Sequences were mapped to the human reference genome (HG19) using the BWA version 0.7.12 (average of mapped reads: 15.7 million, standard deviation: 6.5 million).[19]

Copy-number analysis based on read-count data was conducted using the QDNAseq R package (version 1.10.0) using a fixed window-size of 500 kbp (4407 windows in total).[20] The obtained log2 ratios were smoothed by applying the circular binary segmentation algorithm using the R package copy number version 1.14.0.[21] Based on the absolute log2 ratios observed in the four normal samples (mean + 10*STDEV) the thresholds for calling copy-number gains/losses in the tumor samples were set to 0.09/-0.09, respectively.

A modified chromosomal instability (CNI) score initially developed for the quantification of circulating tumor DNA was used for the comparison between samples and between groups of samples.[22] In brief, after sequencing, the mapped reads are counted in windows along the chromosomes. The percentages of windows above/below the thresholds were calculated as a general measure of the amount of copy-number aberrations present in each tumor.

Genes with causative impacting deletions or amplifications described in the COSMIC Cancer Gene Census database were extracted for regions with gains/losses present in greater than 10%, greater than 20%, and greater than 25% in the TC, AC, and LCNEC/SCC groups, respectively.[23] The percentages of windows above/below the thresholds (CNI score) were calculated as a general measure of the amount of copy-number aberration present in each tumor.

Next-Generation Sequencing

The Human GeneRead DNAseq Targeted Panel V2 (Cat. No.NGHS-003, Qiagen, Hilden, Germany) was processed according to the manufacturers protocol. Briefly, DNA was isolated from 11 LCNECs as described above. The DNA was quantified using the Qubit Assay (ThermoFisher Scientific, Dreieich, Germany) and multiplex polymerase chain reaction (PCR) was performed. DNA amplicons were purified with the AmPure Beads (Qiagen). DNA was end-repaired and adenylated (A-addition) using the GeneRead DNA Library I Core Kit (Qiagen). To each sample a specific QIAseq 12-Index I adaptor (Cat. no. 333714, Qiagen) compatible for Illumina platforms was ligated using the GeneRead DNA Library Core Kit (Qiagen) followed by a purification step with AmPure Beads. The libraries were then size-selected and PCR amplified using the GeneRead DNA Amp Kit. Samples were measured, diluted, and pooled for subsequent sequencing on the Mi-Seq system using the MiSeq Reagent Kit v2 (Illumina MS-102-2002). For data analysis the FastQ files were analyzed in CLC Biomedical Workbench (Qiagen) using an in-house workflow. The reads were mapped on hg19 followed by an initial variant calling. Then local realignments, primer clipping, and low-frequency variant calling were performed. False-positives were removed based on the read quality and the forward/reverse balance. All variants called were checked manually for sequencing artefacts. The average coverage was greater than 500 in all samples; the mutations had at least 50 variant reads.

Sanger Sequencing

Sanger sequencing for neurofibromin 1 (*NF1*) mutation validation was performed using NF1 FOR: 5′- ACT GAC CTT ATG CTT ACT ATT GAG - 3′ and NF1 REV: AAG GTC TTG GCG TTT CAG C as primers. PCR amplification was verified on the QIAxcel Advanced Instrument (Qiagen) and purified using the ExoSAP-IT PCR Product Cleanup (Applied Biosystems). Cleaned-up PCR products were labeled by dideoxynucleotide chain termination using the BigDye Terminator v3.1 Cycle Sequencing Kit and subsequently purified using the BigDye XTerminator Purification Kit (Applied Biosystems) before separating the sequences by capillary electrophoresis on a 3500 Genetic Analyzer (Applied Biosystems). The sequences were compared to an *NF1* reference sequence and analyzed using the software Geneious 11.0.4 (Biomatters Ltd., Auckland, New Zealand).

Statistical Analysis

Statistica version 13.1 (StatSoft Europe, Hamburg, Germany) was used for statistical analyses. Survival analysis was performed via the Kaplan-Meier method and calculated with log rank tests. For direct comparison between two groups, one-way analysis of variance (ANOVA) and Student's *t* test were applied. Associations between potential survival predictors and survival were determined using log rank test. Diagnostic tests to define cutoffs were performed using the Youden index and receiver operating characteristic curve analyses. *p* values less than 0.05 were considered significant.

Results

Clinicopathologic Findings and Application of Different NET Classification Systems

The histopathologic features and the available clinical features of the TNET cohort used in this study are summarized in Table 1. The median age of all patients was 54 years at the time of diagnosis. Of the 107 cases, 22 (20%) were classified as TC, 51 (47%) as AC, 28 (26%) as LCNEC, and 6 (6%) as SCC. TC and AC showed the expected strong predilection for males. Follow-up and survival data were available from 51 patients. The median follow-up time was 52.2 months (range, 1–228 mo). During this period, 25 patients died from their tumor and 26 patients were still alive. Application of the Ki-67–based ENETS classification led to a switch of the risk group (up- or downgrade) of 33% (23 of 69) evaluable cases and application of the three-tiered system according to Pelosi et al.[5] led to a switch in 18% (11 of 60) of evaluable cases (Table 2).

Table 2. Major Morphologic and Immunohistochemical Features of Included Cases and Grouping According to Different Classification Schemes[a]

	WHO TC (n = 22)	WHO AC (n = 51)	WHO LCNEC (n = 28)	WHO SCC (n = 6)
Mitoses range per 2 mm^2 (mean)	0-1 (0.3)	2-10 (4.8)	11-100 (17)	40-105 (81.7)
Necrosis (yes/no)	No	40Y, 10N	21Y, 7N	6Y
Ki-67 index (mean)	0.7-13 (3.3)	1-18.8 (3)	16-90 (54.5)	60-69 (64.5)
ENETS grouping[a]				
NET G1	11	10	0	0
NET G2	5	18	3	0
LCNEC	0	5	11	0
SCC	0	0	0	6
ICPNET				
G1	20	9	0	0
G2	0	21	5	0
G3	0	0	2	3

[a]Not all cases were available for all analyses.
TC, typical carcinoid; AC, atypical carcinoid; LCNEC, large cell neuroendocrine carcinoma; SCC, small cell carcinoma; NET, neuroendocrine tumor; ICPNET, integrated classification of pulmonary NET according to Pelosi et al.[5]; ENETS, European Neuroendocrine Tumor Society.

Genomic Findings

Low coverage whole-genome sequencing (WGS) was possible in 63 cases (13 TC, 30 AC, 16 LCNEC, and 4 SCC). For comparison between cases and groups, the CNI score was used as a measure of overall genomic instability. The average CNI increased from 5.25 in TC to 18.3 in AC to 44.4 in high-grade tumors (LCNEC and SCC) (Fig. 1*A*). There were two notable outliers: one atypical carcinoid with a CNI of 97.7 (Supplementary Fig. 1) and one LCNEC with a CNI of only 3.1. Large copy number alterations were few in TC and included gains on chr. 1q, 5, 6q, 7q, 8q, 10, 11q, 12q, 13q, 18q, 20, 21q, and 22q, and losses on chr. 1, 2p, 4p, 8, 10p, 11p, 15q, 17p, 18p, and 22q. TC and AC showed few overlapping alterations, which included gains on chr. 1q, 7q, 10, 12q, 21, and 22, and losses on chr. 1p, 2p, 4p, 10p, 11p, and 17p. In contrast, the overlap between AC and high-grade tumors (LCNEC and SCC) was extensive: private alterations in high-grade tumors included only gains on chr. 1p, 3p, 11q, and 17q and losses on chr. 1q, 7p, 8q, 14q, 15p, and 15q. 11q deletions, which have been reported as a frequent finding in pulmonary TC and AC, were not found in TNET.[11] Moreover, copy number alterations in gene loci of tumor suppressor and driver genes with reported frequent alterations in PNET were very rare in TC, showed intermediate frequency in AC, and a high percentage in LCNEC/SCC (Supplementary Table 1).[24-26]

Cluster Analysis of Cases Versus Chromosomal Alterations Reveals Three Major Molecular Clusters

Unsupervised clustering of copy number alterations resulted in three major clusters (Fig. 1*B*). Cox proportional hazards regression was used to define CNI cutoffs between the clusters and determined a CNI less than 9 as cutoff for cluster 1 (CNI_{low}) ($p = 0.017$), a CNI greater than or equal to 9 to less than 30 as cutoff for cluster 2 (CNI_{int}), and a CNI greater than or equal to 30 as cutoff for cluster 3 (CNI_{high}). Cluster 3 contained all four SCCs and nine LCNECs, but also three ACs. CNI_{int} cluster 2 and CNI_{low} cluster 1 contained AC and TC, but also six LCNEC cases. Morphology, mitotic count and Ki-67 index showed significant overlap between the three clusters and were unable to predict the CNI cluster (Table 3).

Further analysis was performed of the four cases that had more than one material available (Supplementary Fig. 2). In case 1, the primary tumor was an LCNEC (16 mitoses per 10 HPF; Ki-67, not

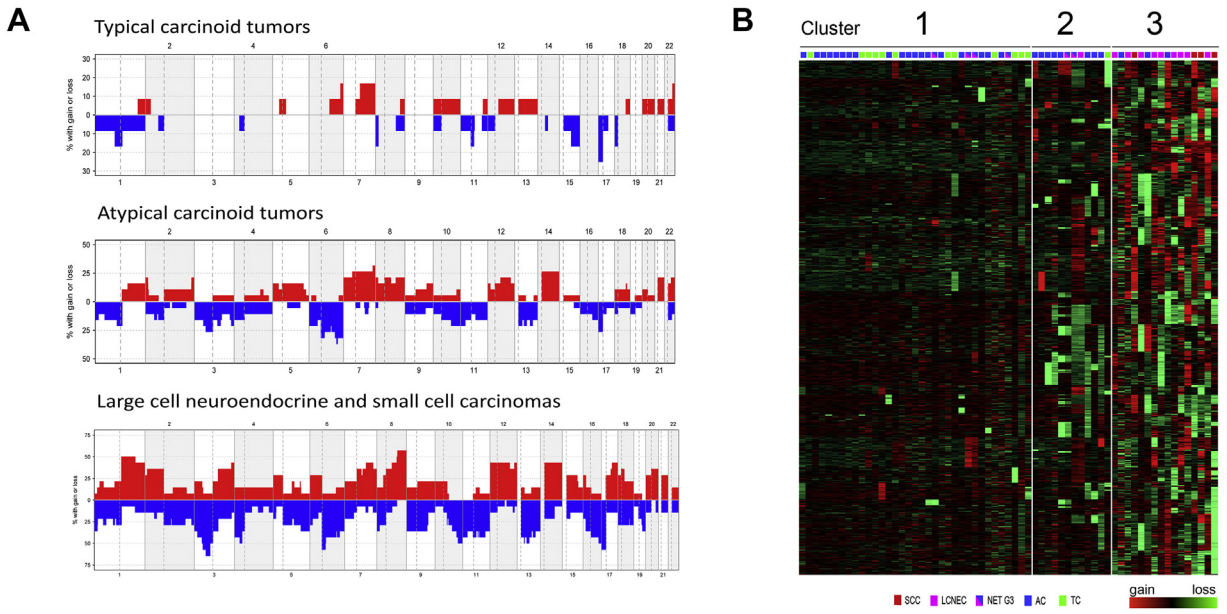

Figure 1. (*A*) Chromosomal gains (*red*) and losses (*blue*) in thymic as detected by shallow whole genome sequencing. Y axis shows percentage of cases with a given chromosomal alteration. (*B*) Unsupervised clustering of whole-genome sequencing data versus WHO histologic subtypes resulted in three major molecular clusters. Cluster 1 contained most of the typical (TCs) and atypical carcinoids (ACs), but also a few large cell neuroendocrine carcinomas (later reclassified as NET-G3). Cluster 2 contained mostly AC, but also an NET G3 and an LCNEC and one TC. Cluster 3 contained all small-cell carcinomas (SCC) and most of the LCNECs, but also three ACs.

available), whereas a synchronous metastasis was classified as AC (seven mitoses per 10 HPF; Ki-67 index, 10.3). Both tumors fell into the CNI_{low} cluster 1 and did not show major molecular differences. After further investigations, the LCNEC was later reclassified as NET G3 (see below). In case 2, the primary tumor was an AC (four mitoses per 10 HPF; Ki-67 index 2.6), whereas a metastasis 3 years later was classified as LCNEC (16 mitoses per 10 HPF; Ki-67 index, 17.5; later reclassified as NET G3). A comparison of primary and metastasis revealed that the latter had acquired a few additional focal chromosomal gains and losses and that both were in the CNI_{low} cluster 1. Case 3 had two samples obtained from the primary tumor (PT1 and PT2) and one metastasis after 5 years. PT1 was classified as TC (0 mitoses; Ki-67 index, 1), PT2 was classified as AC (10 mitoses per 10 HPF; Ki-67 index, 11.9), and the metastasis was classified as LCNEC (16 mitoses per 10 HPF; Ki-67 index, 16; later re-classified as NET G3). PT2 and the metastasis shared many chromosomal gains and losses that were not seen in PT1. PT1 was in CNI_{low} cluster 1, PT2 and the metastasis in CNI_{int} cluster 2. All three samples shared gains on chr. 1.

Table 3. Distribution of Histologic and Immunohistochemical Features of TNET After Assignment to Molecular Clusters

Molecular Cluster	No. Mitoses Range (Median)	Ki-67 Index Range (Median)	CNI Score Range (Median)	WHO	ENETS	Pelosi et al.[5]
CNI_{low} <9	0-27 (3.5)	1-19[a] (7.2)	0-8.8 (5.8)	12 TC 19 AC 4 LCNEC	11 NET G1 10 NET G2	10 G1 11 G2
CNI_{int} ≥9 to <30	0-25 (9.1)	1-14.1[a] (26.1)	9-29.5 (14.6)	1 TC 8 AC 3 LCNEC	8 NET G1 9 NET G2	7 G1 9 G2
CNI_{high} ≥30	0-100 (57.7)	3.5-90 (72.2)	30-97.7 (68.6)	3 AC 9 LCNEC 4 SCC	5 NET G2 9 NEC 4 SCC	1 G1 5 G2 4 G3

[a]Not all cases were available for Ki-67 index staining.

TC, typical carcinoid; AC, atypical carcinoid; LCNEC, large-cell neuroendocrine carcinoma; SCC, small-cell carcinoma; TNET, thymic neuroendocrine tumor; CNI, chromosomal instability score; ENETS, European Neuroendocrine Tumor Society.

Case 4 had two samples obtained from the primary tumor (PT1 and PT2), both were classified as LCNEC (PT1: 12 mitoses per 10 HPF; Ki-67 index, 70; PT2: eight mitoses per 10 HPF; Ki-67 index, 70), and both localized to CNI_{int} cluster 2.

WHO LCNEC Comprise an NET G3 Subgroup

Given the significant "cluster infidelity" of morphologic TNET subtypes, we next analyzed five of the LCNEC cases that had localized to the CNI_{low} and CNI_{int} clusters (hereafter designated NET G3) with sufficient material available and compared them to six LCNEC cases from the high CNI cluster using IHC and targeted deep sequencing (Table 4 and Supplementary Fig. 3).

Presumptive NET G3 cases in the low/intermediate cluster usually had carcinoid morphology (Supplementary Figs. 2*B* through *E*), whereas 3 of 6 cases in the CNI_{high} cluster had a carcinoma (high-grade) morphology. Average mitotic count, Ki-67 index, and CNI score were significantly lower ($p = 0.015$, one-way ANOVA test). We applied a panel of antibodies reported to differentiate GEP–NET G3 from NEC, namely, ATRX chromatin remodeler (ATRX), death domain associated protein (DAXX), SSTR2A, RB transcriptional corepressor 1 (RB), and tumor protein p53 (P53). NET G3 cases showed uniform expression of ATRX, variable expression of DAXX, weak expression of SSTR2A, preserved expression of RB, and wild-type staining of P53.[27] LCNEC cases showed uniform expression of ATRX and DAXX and were negative for SSTR2A. Three of six cases were negative for RB and showed overexpression of P53. Strong overexpression of P53 protein can be an indication for an underlying loss-of-function mutation with consecutive accumulation of nonfunctional protein.

In addition to the observations described in the previous paragraph, we found that two other markers, chromogranin and EZH2, were highly useful to distinguish between NET G3 and LCNEC: chromogranin was positive in all NET G3, but negative in five of six LCNEC. Vice versa, EZH2 was negative in all NET G3, but positive in five of six LCNEC. Synaptophysin was uniformly positive in both groups.

Next, we examined whether chromogranin and EZH2 stains could be used as surrogate markers to predict CNI groups. Cases in the CNI_{low} and CNI_{int} group were 100% (30 of 30) positive for chromogranin and 100% (32 of 32) negative for EZH2. Cases in the CNI_{high} group were 60% (6 of 10) negative for chromogranin and 85% (six of seven) positive for EZH2. Expression of EZH2 in

Table 4. Comparison of Cases Initially Categorized as LCNEC According to WHO but Falling Into the CNI_{low} and CNI_{int} (NET G3) Versus CNI_{high} Cluster (LCNEC)

	NET G3 (n = 5)	LCNEC (n = 6)
Morphology	Low grade	Low or high grade
Mitotic count range per 2 mm^2 (mean)	11-27 (16.8)	12-100 (43.4)
Ki-67 index range (mean)	15-66 (29.5)	52-90 (66)
Immunohistochemical features		
ATRX	Positive (100%)	Positive (100%)
DAXX	Variable (-/(+)/+)	Positive
SSTR2A	Weakly positive	Negative
Retinoblastoma protein	Variable	Variable
P53 protein	Low (WT staining)	Overexpressed (3/6 cases)
Chromogranin	Positive (100%)	Often negative (4/5 cases)
EZH2	Negative (single cells may be positive)	Positive (4/5 cases)
Molecular features		
CNI range (mean)	3.1-18.8 (9,34)	64-83.4 (73.4)
ATRX	*2785C>G (Q929E)* (1 case)[a] *WT* (4 cases)	*WT* (6 cases)
DAXX	*WT* (5 cases)	*WT* (6 cases)
P53	*215C>G (P72R) SNP* (4/5 cases)	*215C>G (P72R) SNP* (2/6 cases)
NF1	*1446A>G (Y489C)* (5/5 cases)	*1446A>G (Y489C)* (6/6 cases)
KRAS	*35G>T (G12V)* (1 case)[b] *WT* (4 cases)	*WT (6 cases)*
NRAS	*38G>T (G13V)* (1 case)[b] *182A>T (Q61L)* (1 case)[b] *WT* (4 cases)	*182A>T (Q61L)* (1 case) *WT* (5 cases)
EZH2, DNMT3A, RB1, KIT, KMT2A, Jak2, JAK3	*WT* (5 cases)	*WT* (6 cases)

[a]Case was positive for ATRX on immunohistochemistry.
[b]Mutations occurred in the same case.
NET, neuroendocrine tumor; WT, wild-type; CNI, ;LCNEC, large-cell neuroendocrine carcinoma.

TNETs was significantly correlated with poor prognosis ($p = 0.00025$, log rank test) (Supplementary Fig. 4). However, these stains were not helpful to identify the few TC and AC cases in the CNI_{high} cluster.

Targeted panel sequencing unexpectedly revealed pathogenic *NF1 p.Y489C* mutations in all (11 of 11) cases analyzed.[28,29] This finding was confirmed by Sanger sequencing (not shown). Due to the high allelic frequency in 10 of 11 cases (average 75.6%), we cannot exclude that this mutation was germline because normal tissue was not available for comparison. The gene locus of *NF1* on chr. 17q11.2 was unaltered in LCNEC, AC, and TC on low-coverage WGS analysis. There was a single *ATRX p.Q929E* missense substitution mutation in one NET G3, whereas all other cases were wild-type for *ATRX* and *DAXX*. The case with the *ATRX* mutation harbored also three concurrent *RAS* mutations (*KRAS p.G12V*, *NRAS p.G13V*, and *NRAS p.Q61L*). One LCNEC carried another *NRAS p.Q61L* mutation. Despite protein overexpression described above, there were no *TP53* mutations; however, 6 of 11 cases (NET G3 and LCNEC) showed a *c.215C>G* (p.Pro72Arg) single nucleotide variant without clinical relevance according to ClinVar definitions (https://www.ncbi.nlm.nih.gov/clinvar). Other genes with reported mutations in NET, *EZH2,* DNA methyltransferase 3 alpha (*DNMT3A*), *RB1,* KIT proto-oncogene, receptor tyrosine kinase (*KIT*), lysine methyltransferase 2A (*KMT2A*),Janus kinase 2 (*Jak2*), and *Jak3* showed wild-type sequence.[17,30,31]

Proposal for an Integrated Morphomolecular TNET Classification

All four classification systems applied in this study (WHO, ENETS, integrated PNET, and CNI score) identified prognostic risk groups. However, all current systems suffer from important drawbacks. The WHO classification, for instance, was initially developed in lung tumors with only very few data to show that it is also relevant in the thymus. TC and AC on the one hand and AC and LCNEC (according to current criteria) on the other show vastly overlapping morphology, prognosis, and genomic features (Supplementary Fig. 5). The cutoffs to separate these entities are unknown. In addition, we herein have shown that areas corresponding to TC, AC, and LCENC (NET G3) can occur in the same tumor.

WHO, the integrated PNET classification, and the molecular CNI scoring system identified three

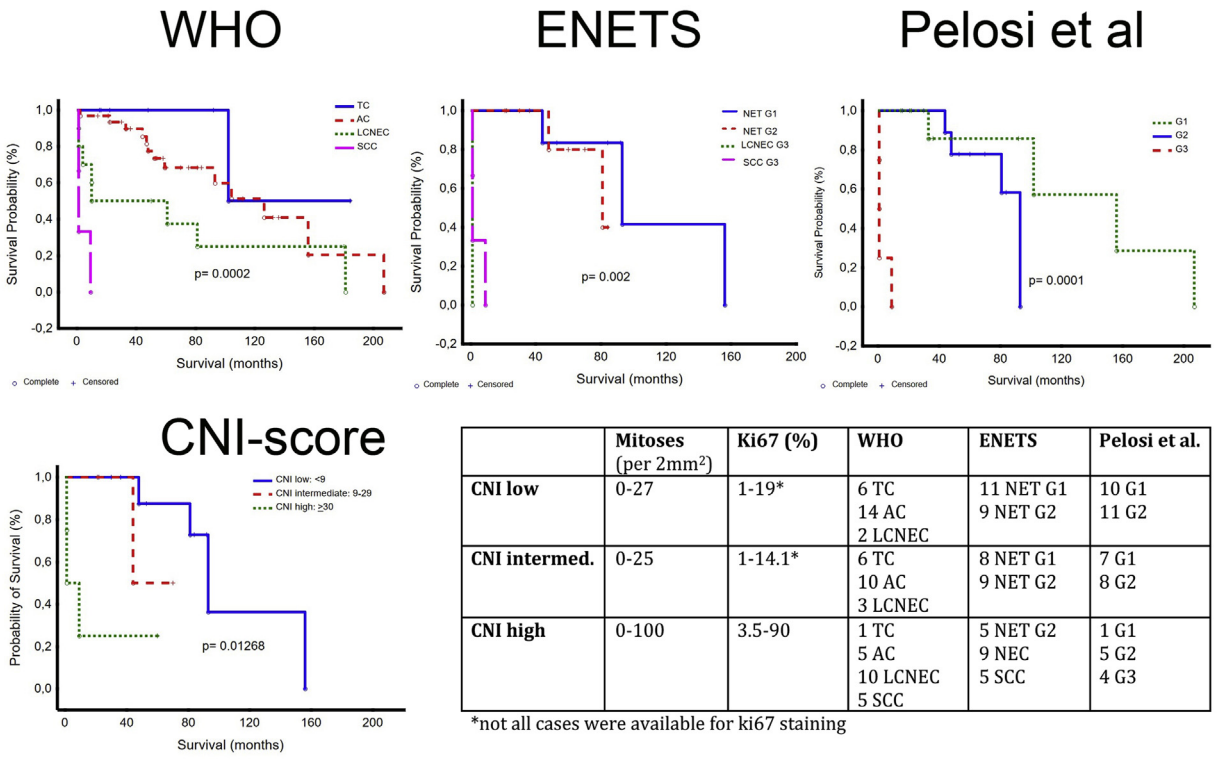

	Mitoses (per 2mm²)	Ki67 (%)	WHO	ENETS	Pelosi et al.
CNI low	0-27	1-19*	6 TC 14 AC 2 LCNEC	11 NET G1 9 NET G2	10 G1 11 G2
CNI intermed.	0-25	1-14.1*	6 TC 10 AC 3 LCNEC	8 NET G1 9 NET G2	7 G1 8 G2
CNI high	0-100	3.5-90	1 TC 5 AC 10 LCNEC 5 SCC	5 NET G2 9 NEC 5 SCC	1 G1 5 G2 4 G3

*not all cases were available for ki67 staining

Figure 2. Prognostic significance and identification of relevant subtypes by morphologic versus molecular TNET classifications. WHO, ENETS, and molecular classification using copy number instability (CNI) score identified three major subtypes (the difference between typical carcinoids, [TC] and atypical carcinoids [AC] in the WHO classification was not statistically significant, log rank test $p = 0.39$), whereas application of the ENETS system resulted only in two subgroups. The table within Figure 2 shows range of mitotic counts, Ki-67 indices, and histologic subtypes according to the three morphologic classifications.

prognostically significant risk groups, whereas ENETS identified only two groups (NET G1/G2 and NEC/SCC) (Fig. 2). Cases that localized to the CNI_{low} cluster 1 invariably had low-grade (carcinoid) morphology, but the CNI_{int} cluster 2 and the CNI_{high} cluster 3 both contained cases with low- and high-grade morphology. Moreover, the current WHO definition does not recognize the newly identified subgroup of NET G3, which would fall either into the low- or intermediate-grade category in a molecular classification. To summarize our morphologic and molecular findings in TNET, we propose a tentative morphomolecular classification by calculating cutoff values with prognostic relevance for all parameters included (Table 5). Analogous to the proposal for an integrated PNET classification by Pelosi et al.,[5] we named the three groups Thy-NET G1-G3. The cutoff values that separated Thy-NET G1 and G2 were less than 10 versus greater than or equal to 10 for mitoses (hazard ratio [HR]: 0.38, $p = 0.03$), less than 9 versus greater than or equal to 9 for Ki-67 index (HR: 0.07, $p = 0.016$), and less than 9 versus greater than or equal to 9 for CNI score (HR: 0.10, $p = 0.047$). The cutoff values that separated Thy-NET G2 from G3 were less than 30 versus greater than or equal to 30 for mitotic counts (HR: 0.02, $p = 0.00023$), less than 48 versus greater than or equal to 48 for Ki-67 index (HR: 0.15, $p = 0.033$), and less than 30 versus greater than or equal to 30 for CNI score (HR: 0.11, $p = 0.018$). The features that characterize the three groups are summarized in Table 5. Since the CNI score is an important feature in this classification, a substantial proportion of cases will be misclassified when using histology and immunohistochemistry alone. In our study, morphologic features without CNI score misclassified 8 of 34 (23.5%) Thy-NET G1 cases as Thy-NET G2, and 10 of 13 (77%) Thy-NET G2 cases as Thy-NET G1. Most critically, while high-grade (carcinoma) morphology, high proliferation, negativity for chromogranin, or expression of EZH2 are strong markers that unambiguously qualify cases as Thy-NET G3, absence of these markers does not rule out a high degree of chromosomal instability in an NET. In our collective, all three carcinoids in the CNI_{high} cluster (including the highly aberrant case) showed low-to-moderate proliferation, were negative for EZH2 and positive for chromogranin, and would have been misclassified as either Thy-NET G2 or even G1.

Discussion

This study on the morphologic and molecular features of TNET established several new findings that lead to a better understanding of these tumors. The most important observation was the fact that TNETs fall into three major molecular subgroups with prognostic relevance, based on a CNI scoring system using low coverage WGS data. The morphologic classifications applied here also showed only three major prognostic groups. A detailed study of the few TNET cases in which primary tumors and metastases could be studied provided further interesting insights. Cases with metachronous metastases showed evidence of morphologic (e.g., switch from AC to NET G3 and increase of mitotic rate and/or mitotic index) and genomic progression (switch from one CNI cluster to another), confirming the previous notion that some NET can either coexist or progress from low- to higher-grade tumors (nominally classified as LCNEC according to current terminology) through acquisition of genomic alterations.[17] Further studies are required to establish whether progression from low-/intermediate- to high-grade tumors, which has been postulated in the lung, also occurs in the thymus.[32]

Another major finding of this study was the identification of a new subgroup of TNET of intermediate grade within the group of LCNEC that we provisionally termed NET G3 in analogy to the terminology in GEP-NET.[7] These NET G3 cases invariably had carcinoid morphology and on average lower mitotic count and Ki-67 indices than (high-grade) LCNEC. On IHC, they expressed ATRX, variably DAXX, were positive for SSTR2A, and showed retained expression of RB and P53

Table 5. Proposal for a Morphomolecular Classification of TNET

Morphomolecular Group	Morphology WHO Subtype	Mitotic Count (per 2 mm^2 or 10 HPF)	Ki-67 Index	CNI Score	IHC
Thy-NET G1	Carcinoid (TC, AC, NET G3)	<10	<9	<9	CGA pos EZH2 neg
Thy-NET G2	Carcinoid or carcinoma (TC, AC, NET G3, LCNEC)	10-29	9-47	9-29	CGA pos EZH2 neg
Thy-NET G3	Carcinoid or carcinoma (LCNEC, SCC)	≥30	≥48	≥30	CGA +/-EZH2 pos

TNET, thymic neuroendocrine tumor; HPF, high-power field; CNI, chromosomal instability score; IHC, immunohistochemistry; TC, typical carcinoma; AC, atypical carcinoma; LCNEC, large-cell neuroendocrine carcinoma; pos, positive; neg, negative.

wild-type staining, whereas LCNECs were positive for ATRX and DAXX and negative for SSTR2A and were partially negative for RB and overexpressed P53. The most specific difference between the two groups, however, was positivity for chromogranin and negativity for EZH2 in NET G3 with the reverse pattern in LCNEC. The combination of these two markers proved helpful in the separation of low-/intermediate-grade NET from NEC in general and overexpression of EZH2 was a marker of poor prognosis. EZH2 is a methyltransferase and is the functional component of the polycomb repressive complex 2 and a very potent negative regulator of gene expression.[33] Overexpression of EZH2 in aggressive NET has been noted before in the lung and the gastrointestinal tract.[34,35] It will be important to study if pharmacologic inhibition of EZH2 can be used for the therapy of these highly malignant tumors.

Sequencing of a limited gene panel revealed a single *ATRX p.Q929E* mutation in an NET G3 and an unexpected high frequency of *NF1* mutations in both NET G3 and LCNEC. *NF1* mutations have also been described in pulmonary carcinoids and in pheochromocytomas, albeit at much lower frequency.[36,37] Somatic *NF1* mutations occur in many sporadic cancers including lung 4cancer, melanoma, ovarian carcinoma, and pheochromocytoma.[37,38] Due to the lack of normal control tissues, we could not differentiate between *NF1* somatic and germline mutations. However, given the high allelic frequency of the mutation in most tumors (>80% in 10 of 11 cases), we cannot exclude an attenuated variant of neurofibromatosis type 1. (Neurofibromin, the protein encoded by the *NF1* gene, is a negative regulator of RAS/mitogen-activated protein kinases (MAPK) signaling and loss of NF1 leads to resistance against BRAF and EGFR inhibitors.[39] The observation that several cases had additional *KRAS* and *NRAS* proto-oncogene, GTPase (*NRAS*) mutations indicates an important role of (or even addiction to) the RAS/MAPK signaling pathway in these tumors that merits further investigation.

The correlation between the molecular subgroups described above and the three histomorphologic classification systems applied here (WHO for PNET and TNET, ENETS system for GEP NET, integrated classification for PNET) was only moderate. Although two of the three histomorphologic classification systems (WHO for PNET and TNET, and the integrated classification for PNET) showed prognostic significance and mirrored the three molecular clusters on a per group basis (e.g., median mitotic count/Ki-67 3.5/7.2 in the CNI_{low} cluster versus 9.1/26.1 in the CNI_{int} versus 57.7/72.2 in the CNI_{high} group) they were unable to correctly assign tumors on a per case basis because all three molecular subgroups were heavily contaminated by cases that would otherwise have been assigned to different risk groups based on morphology and mitotic rate alone. Extreme examples in this respect were the two observed outliers: one AC with a CNI of 97.7 and one LCNEC with a CNI of 3.1. Highly aberrant carcinoids including cases with chromothripsis have also been described in the lung and in other organs and have been attributed to inactivating mutations of polymerase theta (*POLQ*).[24,26,40] Although morphologic features are currently the backbone of TNET classifications, our data indicate that morphology alone will not be sufficient to safely stratify individual patients for clinical purposes. We therefore propose a tentative, three-tiered integrated morphomolecular classification of TNET that is mainly based on molecular features and proliferation rate (Table 5). In an analogy to GEP-NET, where a Ki-67 index of greater than or equal to 55% denotes a clinically important threshold for the decision to use platinum-based chemotherapy, we hypothesize that the potentially most relevant distinction will be the separation of Thy-NET G1/G2 from G3, that is, tumors with greater than or equal to 30 mitoses per 2 mm^2 or a Ki-67 index with a decisional cutoff around 48% to 55%, positivity for EZH2, and loss of chromogranin expression.[41]

We propose this approach for the following reasons: all morphologic classifications applied here (including WHO) identified three prognostic risk groups, suggesting that the three clusters that were detected by genomic findings represent three relevant biologic TNET entities. As a consequence, it would be important to assign individual cases to one of these entities with clinically actionable precision. Importantly, however, we here show that all published morphologically classifications are unable to resolve the vast grey zone especially between AC and LCNEC (as defined by current WHO criteria) on the one hand and between LCNEC/NET G3 and true high-grade LCNEC/SCC on the other. In an extreme (and exaggerated) scenario, according to current criteria, a tumor with 11 mitoses would have to be classified as AC and the patient would be treated according to guidelines for low-grade NET. The same tumor with 11 mitoses would have to be classified as an LCNEC and the patient would be at risk to receive a highly toxic treatement used for small-cell cancers. Finally, as shown here, areas corresponding to TC, AC, and even "LCNEC" (NET G3 according to our definition) can occur in the same tumor. We therefore propose to acknowledge these facts by introducing a provisional three-tiered morphomolecular Thy-NET G1-G3 classification, although this system has important practical limitations (because sophisticated molecular methods are required for its correct application). However, this classification could be a working basis to guide further research, for example, to identify more surrogate

markers such as chromogranin and EZH2 that help to refine morphologic and IHC criteria.

In summary, this study provides strong evidence that TNETs fall into three molecular categories that cannot be reliably reproduced by morphology alone. Tumors so far classified as TC, AC, or the newly defined NET G3 are most likely not true separate entities, but rather a spectrum of tumors that fall into the low- and intermediate-grade molecular categories. Most likely, morphologic and molecular progression can occur within this heterogeneous group. In contrast, true LCNECs fall either into the intermediate- or high-grade molecular category. SCCs always fall into the high-grade category. Further studies will be required to formally investigate if progression from differentiated NET to undifferentiated neuroendocrine carcinoma is also possible.

In conclusion, our data indicate that the biology of TNET is better reflected by a three-tiered morphomolecular grading system than by traditional histologic classifications. Finally, this study showed that the rare TNET share many of the principal features of NET in other organs, justifying a unifying interpretation of these tumors regarding developmental mechanisms or the adaptation of emerging general criteria defined in other organs. Recent molecular studies in PNET, for example, failed to identify any genetic differences between typical and atypical carcinoids.[24] However, our data also revealed some organ-specific features of TNET. It will be important to further characterize these shared and unique features especially for therapeutic purposes and patient stratification.

Acknowledgment

The views expressed in this article are those of the authors and do not reflect the official policy of the Department of Army/Navy/Air Force, Department of Defense, or the U.S. Government.

Supplementary Data

Note: To access the supplementary material accompanying this article, visit the online version of the *Journal of Thoracic Oncology* at www.jto.org and at https://doi.org/10.1016/j.jtho.2019.04.015

References

1. Strobel P, Marx A, Chan JK, et al. Thymic neuroendocrine tumours. In: Travis WD, Brambilla E, Burke AP, et al., eds. *WHO Classification of Tumours of the Lung, Pleura, Thymus and Heart*. Lyon, France: IARC press; 2015:234-241.
2. Moran CA, Suster S. Neuroendocrine carcinomas (carcinoid tumor) of the thymus. A clinicopathologic analysis of 80 cases. *Am J Clin Pathol*. 2000;114:100-110.
3. Gaur P, Leary C, Yao JC. Thymic neuroendocrine tumors: a SEER database analysis of 160 patients. *Ann Surg*. 2010;251:1117-1121.
4. Filosso PL, Yao X, Ahmad U, et al. Outcome of primary neuroendocrine tumors of the thymus: a joint analysis of the International Thymic Malignancy Interest Group and the European Society of Thoracic Surgeons databases. *J Thorac Cardiovasc Surg*. 2015;149:103 e2-109 e2.
5. Pelosi G, Pattini L, Morana G, et al. Grading lung neuroendocrine tumors: controversies in search of a solution. *Histol Histopathol*. 2017;32:223-241.
6. Rindi G, Arnold R, Bosman FT, et al. Nomenclature and classification of neuroendocrine neoplasms of the digestive system. In: Bosman FT, Carneiro F, Hruban RH, et al., eds. *WHO Classification of Tumours of the Digestive System*. Lyon, France: IARC Press; 2010:13-14.
7. Basturk O, Yang Z, Tang LH, et al. The high-grade (WHO G3) pancreatic neuroendocrine tumor category is morphologically and biologically heterogenous and includes both well differentiated and poorly differentiated neoplasms. *Am J Surg Pathol*. 2015;39:683-690.
8. Rindi G, Klimstra DS, Abedi-Ardekani B, et al. A common classification framework for neuroendocrine neoplasms: an International Agency for Research on Cancer (IARC) and World Health Organization (WHO) expert consensus proposal. *Mod Pathol*. 2018;31:1770-1786.
9. Pelosi G, Sonzogni A, Harari S, et al. Classification of pulmonary neuroendocrine tumors: new insights. *Transl Lung Cancer Res*. 2017;6:513-529.
10. Teh BT, Hayward NK, Walters MK, et al. Genetic studies of thymic carcinoids in multiple endocrine neoplasia type 1. *J Med Genet*. 1994;31:261-262.
11. Walch AK, Zitzelsberger HF, Aubele MM, et al. Typical and atypical carcinoid tumors of the lung are characterized by 11q deletions as detected by comparative genomic hybridization. *Am J Pathol*. 1998;153:1089-1098.
12. Ullmann R, Petzmann S, Klemen H, Fraire AE, Hasleton P, Popper HH. The position of pulmonary carcinoids within the spectrum of neuroendocrine tumors of the lung and other tissues. *Genes Chromosomes Cancer*. 2002;34:78-85.
13. Zhao J, de Krijger RR, Meier D, et al. Genomic alterations in well-differentiated gastrointestinal and bronchial neuroendocrine tumors (carcinoids): marked differences indicating diversity in molecular pathogenesis. *Am J Pathol*. 2000;157:1431-1438.
14. Petzmann S, Ullmann R, Klemen H, Renner H, Popper HH. Loss of heterozygosity on chromosome arm 11q in lung carcinoids. *Hum Pathol*. 2001;32:333-338.
15. Johnen G, Krismann M, Jaworska M, Muller KM. [CGH findings in neuroendocrine tumours of the lung]. *Pathologe*. 2003;24:303-307 [in German].
16. Strobel P, Zettl A, Shilo K, et al. Tumor genetics and survival of thymic neuroendocrine neoplasms: a multi-institutional clinicopathologic study. *Genes Chromosomes Cancer*. 2014;53:738-749.
17. Fabbri A, Cossa M, Sonzogni A, et al. Thymus neuroendocrine tumors with CTNNB1 gene mutations, disarrayed ss-catenin expression, and dual intratumor Ki-67 labeling index compartmentalization challenge the concept of secondary high-grade

neuroendocrine tumor: a paradigm shift. *Virchows Arch*. 2017;471:31–47.
18. Shoji T, Fushimi H, Takeda S, Tanio Y. Thymic large-cell neuroendocrine carcinoma: a disease neglected in the ESMO guideline? *Ann Oncol*. 2011;22:2535.
19. Li H, Durbin R. Fast and accurate short read alignment with Burrows-Wheeler transform. *Bioinformatics*. 2009;25:1754–1760.
20. Scheinin I, Sie D, Bengtsson H, et al. DNA copy number analysis of fresh and formalin-fixed specimens by shallow whole-genome sequencing with identification and exclusion of problematic regions in the genome assembly. *Genome Res*. 2014;24:2022–2032.
21. Nilsen G, Liestol K, Van Loo P, et al. Copynumber: efficient algorithms for single- and multi-track copy number segmentation. *BMC Genomics*. 2012;13:591.
22. Weiss GJ, Beck J, Braun DP, et al. Tumor cell-free DNA copy number instability predicts therapeutic response to immunotherapy. *Clin Cancer Res*. 2017;23:5074–5081.
23. Futreal PA, Coin L, Marshall M, et al. A census of human cancer genes. *Nat Rev Cancer*. 2004;4:177–183.
24. Fernandez-Cuesta L, Peifer M, Lu X, et al. Frequent mutations in chromatin-remodelling genes in pulmonary carcinoids. *Nat Commun*. 2014;5:3518.
25. Derks JL, Leblay N, Lantuejoul S, Dingemans AC, Speel EM, Fernandez-Cuesta L. New insights into the molecular characteristics of pulmonary carcinoids and large cell neuroendocrine carcinomas, and the impact on their clinical management. *J Thorac Oncol*. 2018;13:752–766.
26. Simbolo M, Mafficini A, Sikora KO, et al. Lung neuroendocrine tumours: deep sequencing of the four World Health Organization histotypes reveals chromatin-remodelling genes as major players and a prognostic role for TERT, RB1, MEN1 and KMT2D. *J Pathol*. 2017;241:488–500.
27. Konukiewitz B, Schlitter AM, Jesinghaus M, et al. Somatostatin receptor expression related to TP53 and RB1 alterations in pancreatic and extrapancreatic neuroendocrine neoplasms with a Ki67-index above 20. *Mod Pathol*. 2017;30:587–598.
28. Messiaen LM, Callens T, Roux KJ, et al. Exon 10b of the NF1 gene represents a mutational hotspot and harbors a recurrent missense mutation Y489C associated with aberrant splicing. *Genet Med*. 1999;1:248–253.
29. Ars E, Serra E, Garcia J, et al. Mutations affecting mRNA splicing are the most common molecular defects in patients with neurofibromatosis type 1. *Hum Mol Genet*. 2000;9:237–247.
30. Beasley MB, Lantuejoul S, Abbondanzo S, et al. The P16/cyclin D1/Rb pathway in neuroendocrine tumors of the lung. *Hum Pathol*. 2003;34:136–142.
31. Voortman J, Lee JH, Killian JK, et al. Array comparative genomic hybridization-based characterization of genetic alterations in pulmonary neuroendocrine tumors. *Proc Natl Acad Sci U S A*. 2010;107:13040–13045.
32. Pelosi G, Bianchi F, Dama E, et al. Most high-grade neuroendocrine tumours of the lung are likely to secondarily develop from pre-existing carcinoids: innovative findings skipping the current pathogenesis paradigm. *Virchows Arch*. 2018;472:567–577.
33. Moritz LE, Trievel RC. Structure, mechanism, and regulation of polycomb-repressive complex 2. *J Biol Chem*. 2018;293:13805–13814.
34. Bondgaard AL, Poulsen TT, Poulsen HS, Skov BG. Different expression of EZH2, BMI1 and Ki67 in low and high grade neuroendocrine tumors of the lung. *Cancer Biomark*. 2012;11:123–128.
35. Faviana P, Marconcini R, Ricci S, et al. EZH2 expression in intestinal neuroendocrine tumors. *Appl Immunohistochem Mol Morphol*. 2018. https://doi.org/10.1097/PAI.0000000000000647.
36. Asiedu MK, Thomas CF Jr, Dong J, et al. Pathways impacted by genomic alterations in pulmonary carcinoid tumors. *Clin Cancer Res*. 2018;24:1691–1704.
37. Gieldon L, Masjkur JR, Richter S, et al. Next-generation panel sequencing identifies NF1 germline mutations in three patients with pheochromocytoma but no clinical diagnosis of neurofibromatosis type 1. *Eur J Endocrinol*. 2018;178:K1–K9.
38. Philpott C, Tovell H, Frayling IM, Cooper DN, Upadhyaya M. The NF1 somatic mutational landscape in sporadic human cancers. *Hum Genomics*. 2017;11:13.
39. de Bruin EC, Cowell C, Warne PH, et al. Reduced NF1 expression confers resistance to EGFR inhibition in lung cancer. *Cancer Discov*. 2014;4:606–619.
40. Arana ME, Seki M, Wood RD, Rogozin IB, Kunkel TA. Low-fidelity DNA synthesis by human DNA polymerase theta. *Nucleic Acids Res*. 2008;36:3847–3856.
41. Sorbye H, Welin S, Langer SW, et al. Predictive and prognostic factors for treatment and survival in 305 patients with advanced gastrointestinal neuroendocrine carcinoma (WHO G3): the NORDIC NEC study. *Ann Oncol*. 2013;24, 152-1 EZH2 expression in intestinal neuroendocrine tumors 60.